ELSEVIER

2nd International Conference on Structural Integrity, ICSI 2017, 4-7 September 2017, Funchal, Madeira, Portugal

Intellectual monitoring of artificial ground freezing in the fluid-saturated rock mass

Panteleev I.[a], Kostina A.[a], Zhelnin M.[a], Plekhov A.[a]*, Levin L.[b]

aInstitute of Continuous Media Mechanics of the Ural Branch of Russian Academy of Science, Perm, Russia, poa@icmm.ru
bMining institute, Ural Branch of Russian Academy of Sciences, Perm 614007, Russia

Abstract

The paper is devoted to the development of monitoring system of artificial ground freezing process (ice wall formation) under vertical shaft sinking. The work consists of two parts. The practical part includes the development of real-time spatial distributed temperature monitoring system. The temperature in control boreholes is measured using fiber-optic system Silixa Ultima based on the Raman Effect. The fiber-optic system has a characteristic length of several hundred meters and measures the temperature with the step equaled to 0.25m and precision of 0.1°C. The monitoring system is coupled with thermo-hydro-mechanical model of fluid-saturated poroelastic media. This model is used for numerical simulation of freezing process. The model increases the possibilities of the current state control of the process and allows us to forecast the evolution of ice wall. To illustrate the efficiency of the developed system the examples of real monitoring of artificial ground freezing in the fluid-saturated rock mass and simulation of freezing and defrosting processes are presented.

Keywords: artificial ground freezing, mine shaft, fiber optic cable, monitoring system, numerical simulation

1. Introduction

One of the characteristic features of the modern underground building is an increase in the depth of deposits and, as a consequence, complication of geotechnical conditions. This circumstance is directly connected with the increase

---

in the depth of the opening of unstable fluid-saturated rocks requiring special building methods. One of these methods is artificial ground freezing which is used for vertical shaft sinking. Effectiveness of this technique is confirmed by the long-term experience of its application in Russia and some other countries and is determined by the reliability of the ice wall (IW) with calculated thickness. The basic idea of this method is the creation of the IW on the contour of projected to the sinking of the barrel.

Figure 1 presents the IW formation system and structural diagrams of monitoring system. To form the IW the system of the boreholes is drilled on the contour of projected to the sinking of the barrel. Freezing columns are dropped into each borehole. The freezing station provides a circulation of refrigerant with the temperature up to -20 ^{0}C and cools the surrounding ground.

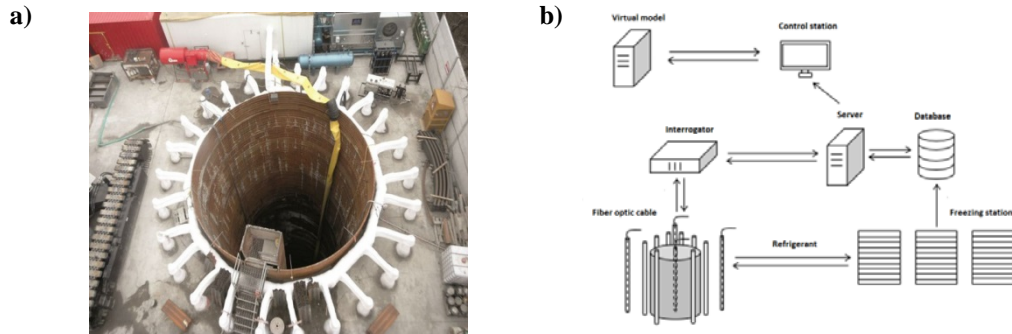**a)**   **b)**

Fig. 1. (a) freezing system (the diameter is 10 m); (b) structural diagram of monitoring system.

The cooling process leads to the water-ice phase transition and emergence of single ice-ground cylinders surrounding each borehole. A merging of the ice-ground cylinders leads to the formation of IW. The mining work can be started after formation of IW with defined thickness. Additionally the real-time monitoring of IW state should be realized during all process of shaft sinking. The monitoring of the process of IW formation is carried out using thermal and hydro measurement borehole, ultrasonic method. The monitoring system should allow one to determine time of IW fencing and calculate its thickness. The analysis of state-of-art in artificial ground frizzing allows us to conclude that temperature measurements do not give enough information to establish the actual parameters of the IW Kazakov et al. (2014).

There are two possible ways to improve the precision of IW control. The first one is an application of modern optical-fiber based spatial distributed temperature measurements system which allows one to monitor in real time several thousand points. The second one is to develop so called "intellectual monitoring system" as proposed in Fedorova et al. (2013). Such system requests a detailed virtual model of the monitoring object and feedback which allows one to treat the recorded data and to simulate the future object behavior.

This work presents a first step for the creation of such system. The virtual model of the monitored object is a thermo-hydro-mechanical model of fluid-saturated poroelastic media. The model was coupled this original monitoring system designed by Mining institute UB RAS. The monitored object is considered as a layered porous media. The media is a three-phased material consisting of a dry skeleton, fluid and ice that completely fill pore space. In the initial configuration porous media is completely filled with water. All liquid transforms into ice and dry skeleton remains unchanged during the phase transition process. The initial temperature data and controlling data were provided by monitoring system. The efficiency of the approach was illustrated by real monitoring of artificial ground freezing process in the fluid-saturated rock mass under sinking salt shafts.

2. Monitoring system

The main elements of the fiber-optical temperature monitoring system are the recorder (interrogator) and optical fiber cable. Fiber optic interrogator is used for generating of the optical signal, the spectral filtering of the light

backscattering, light conversion into electrical signals, amplification and electronic processing. Fiber-optic cable is used as a linear sensor, which is placed in control boreholes for all of their depth.

The cooling effect of the freezing column leads to heterogeneous temperature distribution in surrounding rocks. The optical-fiber system measures the temperature in boreholes with a spatial resolution of 25 cm, temperature accuracy of 0.1 °C and time frequency 1/60 Hz. The temperature measurement is carried out based on the analysis of Raman scattering of light in the optical-fibers. The characteristic temperature evolution under IW formation is shown in figure 2. Additionally the monitoring system controls operation parameters of freezing columns, such as the temperature of direct and reverse flows and flow rate through freezing pipes.
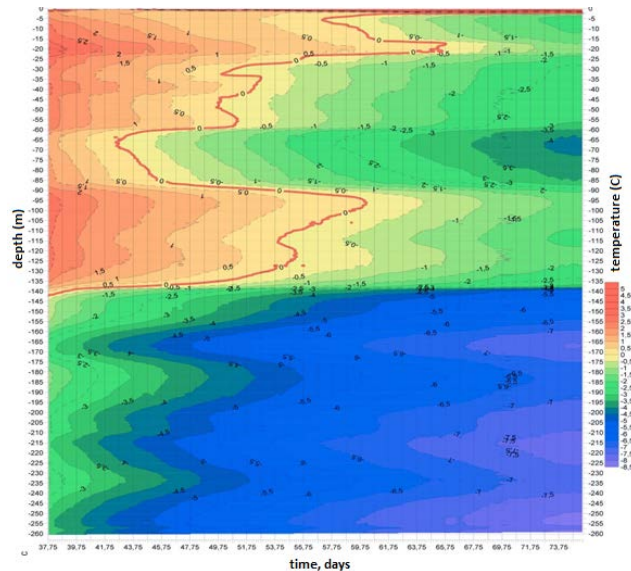

Fig. 2. Temperature evolution in control boreholes.

The developed system allows one to predict the time of the IW formation and to estimate its thickness based on the standard semi-empirical models. But the real process of IW formation is accompanied by unexpected situations that cannot be described in the framework of empirical models. For instance, discrepancy of hydro-monitoring and temperature-measuring data or mismatch of the temperature predicted and measurement temperature into boreholes can be observed. Additional issues associated with the temperature-measuring boreholes spatial arrangement providing a guaranteed monitoring of the state of IW emergence under design of the monitoring system.

A solution of these problems is possible by constructing a mathematical model that predicts temperature distribution in rock masses taking into account phase transitions, geology and hydrogeology data, thermophysical properties of rocks and working parameters of the freezing columns.

3. Numerical simulation of freezing process

Solution to the problem of artificial ground freezing with the use of the direct numerical simulation depends on the two factors: initial data on the thermal and mechanical properties of rocks and adequacy of the used physical model. Artificial ground freezing is a complex multiphasic phenomenon including closely related thermal, mechanical and hydrodynamic processes. Modern physical models which are used in civil engineering, extractive industry, soil science and agricultural engineering can be divided into following groups: rigid-ice models (O'Neill at al. (1985), Sheng et al. (1995)), thermodynamic models (Konrad (1994), Hansson et al. (2004), Nishimura et el. (2009)), semi-empirical models (Nixon (1992)) and poromechanical models (Coussy et al. (2008)). Thermodynamic models can be divided into two classes: freezing models of fully saturated porous media (Mikkola et al. (2001), Kruschwitz et al. (2005)) and models which take into account unfrozen water after phase-transition (Rempel et al.

(2004), Zhou et al. (2013)). Despite the fact that the second-type models describe physical processes of the individual grains and pores more accurately in order to describe phase transition at the large spatial scales it is required separate investigation of unfrozen water on the phase transition rate and coupled filtration-mechanical processes within porous media upon freezing.

The complete three-dimensional formulation of the model under above-described assumptions includes the heat equation (1), the Fourier law (2), the equilibrium equation (3), constitutive equations for the mechanical behavior description (4), the geometric relation for linear strain tensor (5), the continuity equation (6), the Darcy law (7) and can be written in the following form:

$$\rho c_p \frac{\partial T}{\partial t} + \rho_f c_{p,f} \overline{v} \cdot \overline{\nabla} T + \overline{\nabla} \cdot \overline{q} = 0 \qquad (1)$$

$$\overline{q} = -k \overline{\nabla} T \qquad (2)$$

$$\overline{\nabla} \cdot \tilde{\sigma} = \rho \overline{g} \qquad (3)$$

$$\tilde{\sigma} = \tilde{\tilde{C}} : \left(\tilde{\varepsilon} - \tilde{\varepsilon}_T \right) - \alpha_B p_f \tilde{E} \qquad (4)$$

$$\tilde{\varepsilon} = \frac{1}{2} \left[\overline{\nabla}\overline{u} + \left(\overline{\nabla}\overline{u} \right)^T \right] \qquad (5)$$

$$\rho_f S \frac{\partial p_f}{\partial t} + \overline{\nabla} \cdot \left(\rho_f \overline{v} \right) = -\rho_f \alpha_B \frac{\partial \varepsilon_{vol}}{\partial t} \qquad (6)$$

$$\overline{v} = -\frac{k'}{\mu} \left(\overline{\nabla} p_f + \rho_f g \overline{\nabla} z \right) \qquad (7)$$

$$\tilde{\sigma} = \tilde{\tilde{C}} : \left(\tilde{\varepsilon} - \tilde{\varepsilon}_T \right) - \alpha_B p_f \tilde{E} \qquad (8)$$

In (1) – (7): ρ – effective density of the system "dry skeleton – liquid - ice", [kg/m³], c_p – effective heat capacity of the system "dry skeleton-liquid-ice" at constant pressure, [J/kg·K], k – effective thermal conductivity coefficient of the system "dry skeleton-liquid-ice", [W/m·K], T – absolute temperature, [K], $\overline{q}$ – heat flux vector, [W/m²], t – time, [s], ρ_f – fluid density, [kg/m³], $c_{p,f}$ – specific heat of the fluid, [J/kg·K], $\tilde{\sigma}$ – Cauchy stress tensor, [Pa], $\overline{\nabla}$ – Hamiltonian, $\overline{g}$ – acceleration of gravity, [m/s²], $\tilde{\tilde{C}}$ –stiffness tensor, [Pa], which has two components in case of the isotropic linear elasticity (K – bulk modulus, G – shear modulus), α_B – Biot coefficient, $\overline{v}$ – Darcy's velocity, [m/s], p_f – pore pressure of fluid, [Pa], $\tilde{E}$ – unity tensor, $\tilde{\varepsilon}$ – full strain tensor, $\overline{u}$ – displacement vector, [m], $\tilde{\varepsilon}_T$ – thermal strain, ε_{vol} – volumetric part of the full strain tensor, k' – permeability coefficient, [m²], μ – dynamic viscosity of the fluid [Pa·s], z – vertical coordinate, [m], S – fluid loss coefficient defined as $S = n\chi_f + (\alpha_B - \text{n})(1 - \alpha_B)/K_d$, where n – porosity, χ_f – fluid compressibility, [Pa⁻¹], K_d – bulk modulus of the dry skeleton [Pa].

Expressions for density of the considered system taking into account phase transition from state 1 (fluid) to state 2 (ice) and influence of the pore pressure p_f and temperature T have the form:

$$\rho = \theta \rho_{sf} + (1 - \theta) \rho_{si} , \qquad (8)$$

$$\rho_{sf} = \rho_f \left[1 + \alpha_f (T - T_0) + \chi_f p_f \right] n + \rho_s (1 - \text{n}) , \qquad (9)$$

$$\rho_{si} = \rho_i \left[1 + \alpha_i (T - T_0) + \chi_i p_i \right] n + \rho_s (1 - \text{n}) , \qquad (10)$$

where θ characterizes fraction of fluid phase in the material and $(1-\theta)$ – fraction of ice, ρ_s – density of the dry skeleton, [kg/m³], χ_i – ice compressibility coefficient, [Pa⁻¹], ρ_i – ice density, [kg/m³], α_f – thermal expansion coefficient of the fluid, [K⁻¹], α_i – thermal expansion coefficient of ice, [K⁻¹], χ_i – compressibility coefficient of ice, [Pa⁻¹], T_0 – initial temperature, [K].

The following relation was used in order to define effective specific heat at constant pressure:

$$c_p = \frac{1}{\rho}\Big[\theta\rho_{sf}\big\{nc_{p,f}+(1-n)c_{p,s}\big\}+(1-\theta)\rho_{si}\big\{nc_{p,i}+(1-n)c_{p,s}\big\}\Big]+L\frac{\partial\alpha_m}{\partial T}\,, \qquad (11)$$

where $\alpha_m = \dfrac{1}{2}\dfrac{(1-\theta)\rho_{si}-\theta\rho_{sf}}{\theta\rho_{sf}+(1-\theta)\rho_{si}}$, $c_{p,s}$ – specific heat of the dry skeleton, [J/kg·K], $c_{p,i}$ – specific heat of ice, [J/kg·K], L – latent heat, [J/kg].

Effective thermal conductivity was defined as:

$$k = \theta\big\{nk_f+(1-n)k_s\big\}+(1-\theta)\big\{nk_i+(1-n)k_s\big\}\,, \qquad (12)$$

where k_f – thermal conductivity of the fluid, [W/m·K], k_s – thermal conductivity of the dry skeleton, [W/m·K], k_i – thermal conductivity of ice, [W/m·K].

Influence of the θ on the permeability coefficient k' was taken into account with the use of Heaviside function:

$$k'(\theta) = \begin{cases} k', \theta=1 \\ 0, \theta=0 \end{cases}. \qquad (13)$$

Permeability coefficient k' was estimated by the values of the filtration coefficient kf' of every layer, obtained during hydrogeological investigations of this rock mass:

$$k' = \frac{kf'\mu}{\rho g}\,, \qquad (14)$$

where $\mu = 10^{-3}$ – dynamic viscosity of fluid, [Pa·s].

Effect of the volumetric strain, pressure and temperature was taken into account as [4]:

$$n = n_0 + \alpha_B\varepsilon_{vol} + \frac{1}{N}p_f - 3\alpha_s\big(\alpha_B-n_0\big)\big(T-T_0\big)\,, \qquad (15)$$

where N – Biot tangent modulus, [Pa] α_s – thermal expansion coefficient of the dry skeleton, [K⁻¹], n_0 – initial porosity.

As it has been mentioned above, every layer is isotropic. Results of the laboratory studies of the elastic properties K_{si} and G_{si} of water-saturated rock samples under negative temperature were used to define bulk modulus K and shear modulus G of the dry skeleton. Assuming that effective elastic modulus of the frozen rock mass is determined by the mixture rule, elastic modulus of the dry skeleton K and G can be found as

$$K = \frac{K_{si}-nK_i}{1-n}\,,\; G = \frac{G_{si}-nG_i}{1-n}\,,$$

where $K_i = 1.8\cdot10^9\,Pa$, $G_i = 1.4\cdot10^9\,Pa$ – bulk modulus and shear modulus of ice.

The Biot coefficient and the Biot tangent modulus was defined as:

$$\alpha_B = 1 - \frac{K_d}{K}, \quad \frac{1}{N} = \frac{\alpha_B - n}{K},$$

where K_d – bulk modulus of the dry porous skeleton calculated by the formula:

$$K_d = \frac{K}{1 + \dfrac{3(1-\nu)n}{2(1-2\nu)(1-n)}},$$

where $\nu = 9K/2(G+3K) - 1$ – Poisson's ratio of soil particles.

Thermal strain $\tilde{\varepsilon}_T$ was determined according to the equation:

$$\tilde{\varepsilon}_T = \alpha_s \left(T - T_0\right)\tilde{E}. \tag{16}$$

Equations (1)-(16) are supplemented with the following initial and boundary conditions:

$$p_f\left(t = 0\right) = 0, \tag{17}$$

$$\overline{v}\left(t = 0\right) = \overline{0}, \tag{18}$$

$$\overline{u}\left(t = 0\right) = \overline{0}, \tag{19}$$

$$T_i\left(t = 0\right) = T_{o_i}, \ i = 1...n, \tag{20}$$

$$u_x\big|_{\Gamma_j, \Gamma_j} = 0, \ j = 1...m, \tag{19}$$

$$u_y\big|_{\Gamma_j, \Gamma_l} = 0, \ j = 1...m, \tag{21}$$

$$\overline{u}\big|_{\Gamma_b} = \overline{0}, \tag{22}$$

$$\tilde{\sigma} \cdot \overline{n}\big|_{\Gamma_b} = \rho \overline{g} z, \tag{23}$$

$$\tilde{\sigma} \cdot \overline{n}\big|_{\Gamma_u} = \rho \overline{g} z, \tag{24}$$

$$-\overline{n} \cdot \overline{q}\big|_{\Gamma_l, \Gamma_u, \Gamma_b} = 0, \tag{25}$$

$$-\overline{n} \cdot \rho \overline{v}\big|_{\Gamma} = 0, \tag{26}$$

$$T\big|_{\Gamma_j} = T_1\left(t,x\right), \ T_1\left(t,x\right) = -(T_{pod}(t) - T_{obr}(t))x/h_1 + T_{pod}(t), \ j = 1...m \tag{27}$$

where T_{o_i} – initial temperature of the layer, i – layer number, n – number of layers, j – well number, m – number of wells, Γ_j – well boundary, Γ_b – lower boundary of the layer, Γ_u – upper boundary of the layer, Γ_l – boundary of the considered area of layered rock mass, $\Gamma = \Gamma_l \cup \Gamma_b \cup \Gamma_u \cup \Gamma_j$, T_{pod} – temperature of coolant supply, T_{obr} – coolant return temperature, h_1 – depth of freeze wells. It is assumed that pore pressure, Darcy's velocity, initial displacement of the solid skeleton are zero, initial temperature of each layer is known from the geophysical investigations. Horizontal displacements and heat flux on the outer boundaries of the considered area are zero. Lithostatic pressure on the boundaries of the layers corresponds to the given depth. Zero horizontal displacements and linear temperature gradient are prescribed on the walls of the freezing wells. The temperature on the bottom of the wells is equal to the temperature of the coolant supply; the temperature on the wellhead is equal to the return temperature of coolant.

The initial data were generated close to the real observed situation. Artificial freezing zone includes 41 freezing wells. Centers of these wells are located on the circle which has the diameter of 10.5 m and located at the distance of 1608 mm from each other. The diameter of the freezing well is 146 mm and its depth is 225 m. To simulate influence of the real geometry of the wells after drilling, the artificial inclinometer data were generated. Deviation of the bottom of each well from the vertical was taken into account during the simulation.

A real data on the coolant temperature supply and return were used to define boundary conditions. According to the geological data sedimentary cover consists of 30 layers up to a depth of 225 meters. All 30 layers were grouped into 13 layers with similar thermophysical properties and permeability. Averaged properties of each layer were calculated as the arithmetic mean of the physical properties combined in one group.

4. Numerical results

The considered area is a cylinder with a depth of 225 meters and diameter of 26.5 meters. This area has been divided by finite elements which have a form of rectangular prisms. The size of the finite element was 9-11 centimeters in the vicinity of the well and 6-7 meters in the periphery. The height of the elements was no more than 6 meters. The total number of elements was about 1 million.

Figure 3 presents the results of numerical simulation of temperature distribution in the borehole presented in figure 2. The date demonstrates all quantitate peculiarities of temperature distribution in real situation.

Additionally, the mathematical model allows us to reconstruct the geometry of IW in different times. The geometry of IW (position of the phase transition front) is presented in figure 4.
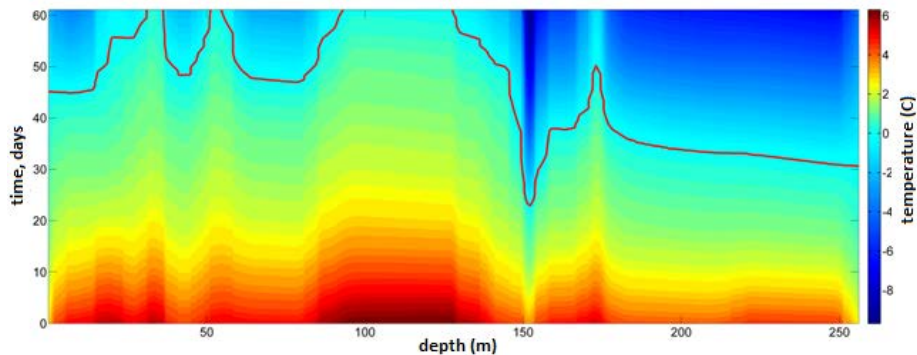

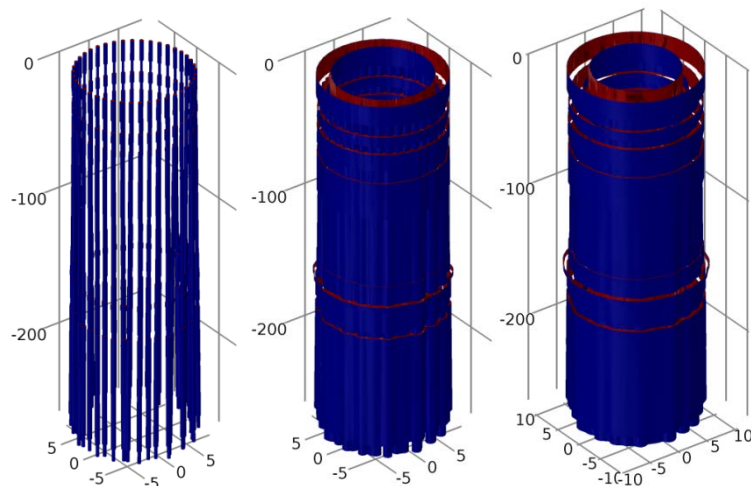Fig. 3. Numerical results of temperature evolution in control boreholes.

Fig. 4. Evolution of the phase transition front (from left to right: day 37, day 112 and day 187).

5. Conclusions

This work is devoted to the development of monitoring system including the measurement part, multiphysics model of artificial ground freezing process and feedback. The multiphysics model includes the solution to the several problems: the problem of non-stationary thermal conductivity with phase transition, the problem of linear filtration and the problem of thermo-elasticity. The first approximation of the model is based on the following hypotheses: isotropy of the physical properties in the rock layers, the absence of the unfrozen water after phase-transition, small deformation of the porous media and weak compressibility of the fluid.

This simplified model was used for the numerical simulation of real industrial process of IW formation in water-infiltrated soil designed for the construction of a vertical mine at one of the potash deposits. Numerical simulation was carried out by the finite-element method. The numerical results have a good qualitative agreement with real monitoring data. The results of numerical simulation allowed us to reconstruct the 3D process of ice formation, define time of the IW closure and estimate the thickness of the IW in each ground layer. It has been shown that non-uniformity of IW is an important factor for providing the safety of mining works. The simulation allows us to model the virtual scenarios of IW formation and recommend the optimal freezing regimes.

Acknowledgements

References

Coussy O, Monteiro PJM, 2008. Poroelastic model for concrete exposed to freezing temperature. Cement and Concrete Research, 38: 40–48.

Fedorova V.A., Matveenko V.P., Shardakov I.N., Tsvetkov R.V. 2013, Intelligent monitoring of mechanical behavior of engineering constructions and natural objects. In: Topical Problems in Theoretical and Applied Mechanics (ed. N.K. Gupta, A.V. Manzhirov, R. Velmurugan). Elite Publishing House PVT LTD, New Delhi, P. 240.

Hansson K, Simunek J, Mizoguchi M, et al., 2004. Water flow and heat transport in frozen soil: numerical solution and freeze-thaw applications. Vadose Zone Journal, 3: 693–704.

Kazakov, B.P., Levin, L.Yu., Zaytsev, A.V., 2014, Modern approaches to development of methods of controlling of thermal mode of mines with high temperature of rock massif. Gornyi Zhurnal 6, 3-56 (in Russain)

Konrad JM, 1994. Sixteenth Canadian geotechnical colloquium frost heave in soils: concepts and engineering. Canadian Geotechnical Journal, 31(2): 223–245.

Kruschwitz J, Bluhm J, 2005. Modeling of ice formation in porous solids with regard to the description of frost damage. Computational Material Science, 3-4: 407-417.

Mikkola M, Hartikainen J, 2001. Mathematical model of soil freezing and its numerical application. International Journal for Numerical Methods in Engineering, 52: 543-557.

Nishimura S, Gens A, Olivella S, et el., 2009. THM-coupledfinite element analysis of frozen soil: formulation and application. Ge-otechnique, 59(3): 159–171.

Nixon JF, 1992. Discrete ice lens theory for frost heave beneath pipelines. Canadian Geotechnical Journal, 29(3): 487–497.

O'Neill K, Miller RD, 1985. Exploration of a rigid ice model of frost heave. Water Resources Research, 21(3): 281–296.

Rempel AW, Wettlaufer JS, 2004. Premelting dynamics in a continuum model of frost heave. Journal of fluid mechanics, 498: 227-244.

Sheng D, Axelsson K, Knutsson S, 1995. Frost heave due to ice lens formation in freezing soils 1. Theory and verification. Hydrology Research, 26(2): 125–146.

Zhou MM, Meschke G., 2013. A three-phase thermo-hydro-mechanical finite element model for freezing soils. International journal for numerical and analytical methods in geomechanics, 37: 3173-3193.